Author Manuscript

Author Manuscript

Author Manuscript

Author Manuscript

HHS Public Access

Author manuscript

Solid State Nucl Magn Reson. Author manuscript; available in PMC 2023 December 01.

Published in final edited form as:

Solid State Nucl Magn Reson. 2022 December ; 122: 101838. doi:10.1016/j.ssnmr.2022.101838.

MAS-DNP Enables NMR Studies of Insect Wings

Frédéric Mentink-Vigier[1], **Samuel Eddy**[2], **Terry Gullion**[2]

[1]CIMAR/NMR National High Magnetic Field Laboratory, 1800 E. Paul Dirac Drive, Tallahassee, Florida 32310

[2]Department of Chemistry, West Virginia University, Morgantown, WV 26506

Abstract

NMR is a valuable tool for studying insects. Solid-state NMR has been used to obtain the chemical composition and gain insight into the sclerotization process of exoskeletons. There is typically little difficulty in obtaining sufficient sample quantity for exoskeletons. However, obtaining enough sample of other insect components for solid-state NMR experiments can be problematic while isotopically enriching them is near impossible. This is especially the case for insect wing membranes which is of interest to us. Issues with obtaining sufficient sample are the thickness of wing membranes is on the order of microns, each membrane region is surrounded by veins and occupies a small area, and the membranes are separated from the wing by physical dissection. Accordingly, NMR signal enhancement methods are needed. MAS-DNP has a track record of providing significant signal enhancements for a wide variety of materials. Here we demonstrate that MAS-DNP is useful for providing high quality one-dimensional and two-dimensional solid-state NMR spectra on cicada wing membrane at natural isotopic abundance.

Graphical Abstract

Correspondence to: Frédéric Mentink-Vigier, fmentink@magnet.fsu.edu, Terry Gullion, terry.gullion@mail.wvu.edu.

Publisher's Disclaimer: This is a PDF file of an unedited manuscript that has been accepted for publication. As a service to our customers we are providing this early version of the manuscript. The manuscript will undergo copyediting, typesetting, and review of the resulting proof before it is published in its final form. Please note that during the production process errors may be discovered which could affect the content, and all legal disclaimers that apply to the journal pertain.

Declaration of interests

The authors declare that they have no known competing financial interests or personal relationships that could have appeared to influence the work reported in this paper.

Author Manuscript Author Manuscript Author Manuscript Author Manuscript

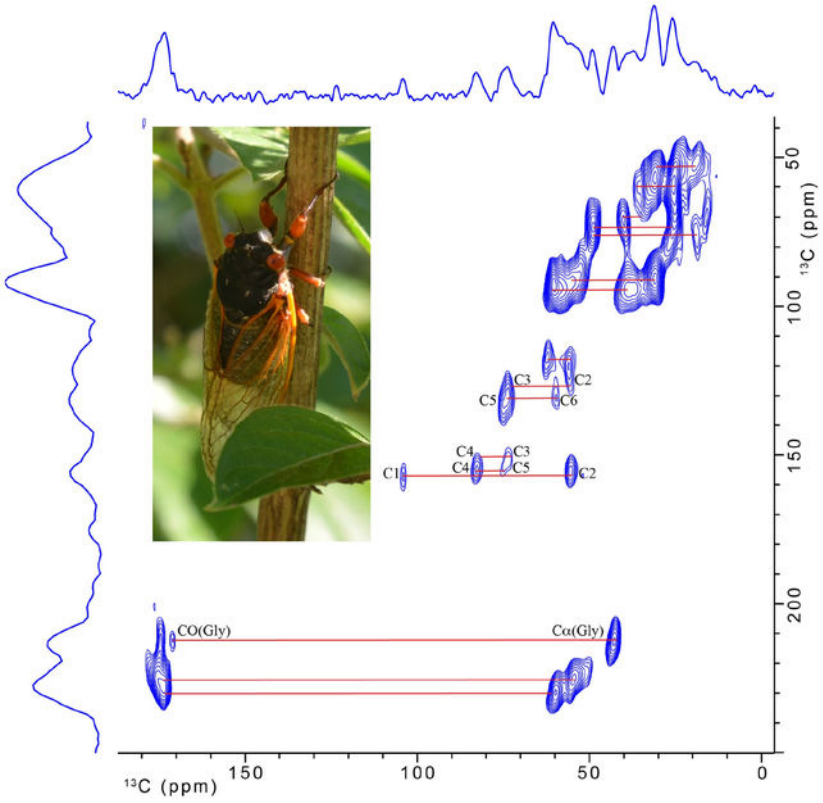

Keywords

MAS-DNP; cicada; insect wing; chitin; NMR

Introduction

Insects are the most diverse group of animals, accounting for over 80% of all species and with a total population of approximately one million trillion [1–4]. Several reasons are attributed to why insects have become so successful, and the most important reason appears to be their ability to fly. Insects were the first animals to fly. Flight provides insects significant advantages in avoiding predators, finding food, finding mates, and populating new areas.

Insect wings are an outgrowth of the exoskeleton [1]. The wing itself is made of a network of veins and thin membranes and must be flexible enough to allow sufficient bending and twisting that is necessary for flight but strong enough to withstand the forces from the repeated flapping motion. The wing is attached to the exoskeleton, and muscles located where the wing and the exoskeleton join are responsible for the active motion of the wing. However, unlike birds and bats, the insect wing has no muscles. Birds and bats use muscles found throughout the wing to control complex flight paths. Since insect wings contain no muscles, the observed flight paths of insects rely partly on passive wing deformations allowed by the wing's flexibility [4, 5].

Author Manuscript Author Manuscript Author Manuscript Author Manuscript

The insect exoskeleton is hard and rigid and serves to support and protect the insect, whereas the wing membrane is tough and flexible. Accordingly, substantial differences between the chemical composition and molecular organization likely exist between the exoskeleton and the wing membrane. Extensive solid-state NMR studies have been performed on insect exoskeletons, with particular focus on sclerotization [6–14]. Only recently has solid-state NMR been used to characterize the wing membrane [15, 16]. The primary difficulty in using NMR to study wing membranes is collecting enough sample. The membrane must be cut from the wing using a knife and magnifying lens, and care must be taken to exclude any material from the veins. Membranes are typically only a few microns thick, so a typical cut over a few square millimeters contains little sample by mass. As an example, dissection of 5000 honeybees yielded only 50 milligrams of membrane sample in a recent study and was a very time-consuming task. ^{1}H-^{13}C CPMAS NMR has been used compare the chemical composition of cicada, honeybee, ladybug, and butterfly wing membranes. The one-dimensional NMR experiments show that the membranes from these insects contain mostly protein and chitin, but not in similar ratios. For example, cicada membrane is protein rich and chitin poor whereas honeybee membrane is chitin rich and protein poor, relatively speaking. Maybe the differences in the ratio of protein to chitin between the insects serves the respective insect's flight requirements.

Acquiring enough sample is the challenge to performing solid-state NMR (ssNMR) on wing membranes, and this is especially true for multi-dimensional NMR experiments. Isotopic enrichment would overcome the sensitivity problem, but isotopic enrichment is near impossible for most insects and cost prohibitive. An alternative is to take advantage of significant signal enhancements using dynamic nuclear polarization combined with magic angle spinning (MAS-DNP) [17–25]. MAS-DNP has demonstrated its incredible usefulness with samples at natural abundance [26–30]. To our knowledge MAS-DNP has not been applied insect samples. A notable concern is how effective MAS-DNP would be for a micron-thick composite system such as insect wing membrane for which the composition can lead to fast relaxing protons, notably due to the presence of methyl groups that can relax quickly. The other issue is how efficient and how homogenous is the nuclear spin hyperpolarization within the wings.

We show that MAS-DNP has the potential to provide significant structural information on insect wings. ^{13}C NMR spectra of the membranes of cicada are presented. The purpose of this paper is to illustrate the potential of MAS-DNP as a good tool for complex, sample-limited insect samples that are not amenable to isotopic labeling. Detailed interpretation of the spectra is reserved for a latter publication.

Experimental

Deceased cicadas (*Magicicada cassini*) were collected in Morgantown, West Virginia during the periodic 17-year emergence that occurred in 2016. No chemical treatments were applied to the insect wing membranes used in this study. Membrane material was extracted from the forewings of the cicada using a knife. Care was taken by obtaining the cuttings with the aid of magnifying glasses to prevent any vein material from contaminating the samples, and

Author Manuscript Author Manuscript Author Manuscript Author Manuscript

final quality control was performed by inspecting the cut membranes under a microscope and discarding any materials that showed any evidence of vein contamination.

Chitin was obtained from cicada sloughs using a modified extraction method described previously [31]. Cicada sloughs were obtained in Knoxville, Tennessee during the seventeen-year 2021 emergence of Brood X. The heads and legs of the cicada sloughs were separated from the bodies of the sloughs and discarded, and only the body (thorax and abdomen) sections were used. The cicada slough bodies were ground in a coffee grinder and then transferred to a 1liter beaker with 750 mL of 2N HCl and stirred for 40 minutes at 100 °C. The beaker was removed from the hot plate to cool, and then the solution and resulting suspended powder were transferred to a Buchner funnel for vacuum filtration. The recovered powder was rinsed thoroughly with ultrapure water. The wet powder was placed in a 500 mL three-neck round-bottom flask. The round-bottom flask was filled with 250 mL, 2N NaOH solution. A condenser was connected to one of the three necks of the flask, a thermometer was inserted in the second neck, and the third was capped off. The 2N NaOH solution was heated at 80 °C for 72 hours. After 72 hours the flask was allowed to cool to room temperature, and the solution and suspended powder, which is chitin, was filtered using vacuum filtration with a Buchner funnel. The recovered chitin was rinsed with ultrapure water and dried in a vacuum oven.

The cross-polarization magic-angle spinning (CPMAS) NMR spectra shown in Figures 1 and 2 were obtained on a custom-built spectrometer using a Tecmag Redstone console and a 3.55 T magnet (proton frequency of 151.395 MHz). The NMR probe is a transmission-line design. It incorporates a Chemagnetics 7.5 mm pencil rotor spinning assembly with a 14-mm long, 8.65-mm inner diameter, 6-turn coil made of 14-gauge copper wire. Radio–frequency (rf) field strengths were 50 kHz for the ^{13}C channel. The ^{1}H rf field strength was 50 kHz for ^{1}H-^{13}C cross-polarization (CP) and 115 kHz for continuous-wave proton decoupling. The rf field strengths for the ^{1}H and ^{13}C channels were determined by measuring the time for a 2π rotation. The ^{1}H and ^{13}C power amplifiers were under active control using a custom-built rf controller. Sample spinning speeds were set to 3600 Hz, and the spinning speeds were actively controlled to within 0.2 Hz of the set point. All NMR spectra were obtained using a spin-echo pulse sequence, with the time between the end of the CP pulse and the refocusing π pulse equal to one rotor cycle. CP contact times were 1 ms and recycle times were 2 seconds for the spectra shown in Figure 1, and each spectrum was acquired in 23 hours. The spectra in Figure 2 were obtained with a 1 ms CP contact time and with recycle delays of 1 second for the cicada sample and 5 seconds for the ladybug and honeybee samples. Preliminary results showed no difference between spectra obtained on cicada with 1 second and 5 second recycle delays. Approximately 50 mg of each membrane sample was used to obtain the spectra. The cicada, ladybug, and honeybee spectra shown in Figure 2 were obtained in 167 hours, 140 hours, and 140 hours, respectively.

The MAS-DNP spectra shown in Figures 3 and 4 were obtained on approximately 10 mg of cicada wing membrane on a system built with a 14.1 T magnet at the National High Magnetic Field Laboratory in Tallahassee, Florida. The cicada wing membrane sample was impregnated with a 30 mM solution of cAsymPol-POK in 10% d6-DMSO/H_2O (1/9 vol %) [32]. The sample was progressively packed into a 3.2 mm sapphire rotor, and the biradical

Author Manuscript Author Manuscript Author Manuscript Author Manuscript

containing solution was added on top at each step of packing. The radical concentration was chosen to reach optimal enhancements in fully protonated media, based on previous work [32]. Each of the MAS-DNP spectra shown in Figure 3 (bottom) were acquired in 128 seconds, and the MAS-DNP DQ/SQ spectrum shown in Figure 4 was acquired in 72 hours.

The sample was first spun at room temperature in a home build benchtop spinner and then an EPR spectrum at room temperature was collected on an EMX Nano benchtop EPR spectrometer to check the biradical's mobility. Then the sample was inserted in the MAS-DNP probe cold (~100 K) and spun at 10.5 kHz. The microwave beam was controlled by a quasi-optic setup and the beam polarization was optimized using a Martin-Puplett interferometer [33, 34]. The sample was irradiated with ~12 W of (μw) power measured at the probe base, which was determined to be optimal. For $^{1}H \rightarrow {}^{13}C$ CP, a 20% ramp CP pulse of duration 600 μs and centered at 50 kHz nutation was applied on the ^{1}H channel and a 39.5 kHz pulse was applied on the ^{13}C channel. All other pulses on the ^{1}H channel were 100 kHz and decoupling was carried out using SPINAL64 [35]. For SPC-5 [36], identical conditions were used except that a CW decoupling of 105 kHz was applied during the recoupling. The excitation duration of the DQ recoupling was set to 570 μs to favor the detection of directly bonded ^{13}C-^{13}C spin pairs.

Results and Discussion

Low Field Results for Insect Wing Membranes and Cicada Exuviae

While our focus is the characterization of insect wing membranes, it is useful to review the ^{13}C CPMAS spectra of the insect exoskeleton as a point of reference. Figure 1 (bottom) shows the ^{13}C CPMAS spectrum of cicada exuviae, and it is similar to the ^{13}C spectra obtained on previously studied insect exoskeletons [6–14] and butterfly chrysalis [37]. The assignments of ^{13}C resonances for insect exoskeletons are provided in Table 1. The dominant components of the cicada exoskeleton are chitin and protein. Additionally, there is significant contribution from catechols, which play a central role in sclerotization, and the ^{13}C resonance associated with catechols at 144 ppm is distinct. The ^{13}C resonances associated with chitin are intense in the spectrum for the exuviae. The ^{13}C CPMAS spectrum of chitin isolated from cicada exuviae is shown in Figure 1 (top). Comparing the spectra in Figure 1 show the ^{13}C resonances for the C1, C3, C4, and C5 carbons of chitin are well resolved from all other resonances, and the ^{13}C resonances for the C2, C4, carbonyl, and methyl resonances of chitin overlap with contributions from protein.

Our prior NMR experiments [15] showed expected resonances from protein and lipid components in the cicada wing membrane, but resonances identifiable to chitin were also observed in the experiments. The finding of chitin in the cicada wing membrane contrasts with the textbook model of the membrane being made of dorsal and ventral epicuticle chitin-free layers [1]. Because of this unexpected result with cicada, we examined the chemical composition of wing membranes for three other insects [16]. We have obtained low-field solid-state NMR results for the wing membrane of cicada (*Magicicada cassini*), honeybee (*Apis mellifera ligustica*), ladybug (*Hippodamia convergens*), and amber phantom butterfly (*Haetera piera*; Peru). Chitin was found in the wing membranes of all four insects, but the relative contribution of chitin to protein varied between insects. The wing membrane

Author Manuscript Author Manuscript Author Manuscript Author Manuscript

of honeybee was the most chitin rich, and the wing membrane of cicada was the most protein rich. Previously described ^{13}C CPMAS spectra taken at low field are shown for the cicada, ladybug, and honeybee wing membrane samples in Figure 2. The ^{13}C resonances for the C1, C3, C4, and C5 carbons of chitin are well resolved from all other resonances in the wing membrane samples. The honeybee wing sample shows evidence for catechols (peak at 144 ppm), but the cicada and ladybug do not show a definite ^{13}C resonance associated with catechols.

Cicada Wing Membrane MAS-DNP Results

The low-field ^{1}H-^{13}C CPMAS NMR experiments on the wing membranes were time consuming, primarily because of the difficulty in obtaining suitable amounts of sample. MAS-DNP has the potential to overcome the problem of limitations in sample quantity for composite insect components for CPMAS experiments and to extend spectroscopic methods to multi-dimensional experiments.

Figure 3 shows ^{1}H-^{13}C CPMAS spectra of the cicada wing membrane obtained on the DNP-equipped spectrometer. The bottom spectrum was obtained with microwaves on, and the top spectrum was obtained without. Each spectrum was obtained with 128 scans. The DNP-off spectrum is scaled by a factor of 5. The enhancement provided by DNP is approximately $\epsilon_{on/off} \approx 22$ for the ^{13}C resonances and the enhancement appears to be similar for the chitin contributions and the protein contributions. Cicada membranes are approximately 4.7 microns in thickness, and the similarities between the two spectra in Figure 3 shows the MAS-DNP enhancement either captures the bulk of the sample and/or the membrane surface chemistry is like the bulk chemistry. However, the saturation-recovery curves could be fitted by a mono-exponential curve with a build-up time of 1.5 s, thereby indicating that the sample can be homogeneously polarized.

A concern with the low field ^{13}C CPMAS cicada wing membrane results was the absence of a resonance around 145 ppm, attributed to cross-linking catechols. The excellent signal-to-noise ratio provided by the MAS-DNP experiment with CP conditions given in the Experimental section appears to confirm that catechols are either not present or are at a very low level compared to the honeybee sample. In addition, the 144 ppm resonance did not appear even when the CP contact time was varied from 100 to 1500 μs, and it did not appear during a multi-CP experiment using seven 100 μs CP pulses with delays of 2 sec [38]. The resolution of the solid-state NMR spectrum under DNP conditions is remarkable. The intrinsic rigidity of the sample may explain why the resolution is maintained under MAS-DNP conditions, as this was observed for instance with amyloids and carbohydrate samples [39, 40]. The excellent signal-to-noise ratio provided by MAS-DNP, with so few scans, suggests that ^{13}C-^{13}C multi-dimensional NMR experiments are possible.

Figure 4 shows the two-dimensional natural abundance ^{13}C-^{13}C double-quantum, single-quantum MAS-DNP NMR spectrum obtained on the 10-mg cicada membrane sample. The signal-to-noise ratio is good. Some of the readily apparent cross-peaks are indicated by the solid lines, and ^{13}C resonances associated with chitin that overlap with protein contributions at 55 and 60 ppm in the 1-D spectrum are now resolved. Assignments and connectivity between all carbons for chitin are easily determined in the spectrum and are labeled

Author Manuscript Author Manuscript Author Manuscript Author Manuscript

according to the numbering scheme shown in Table 1. In addition, there is evidence that glycine makes a significant contribution to the protein as evidenced by the C_α-CO cross-peak of glycine. The additional, unlabeled lines for carbon-carbon cross peaks in the figure serve to further emphasize the high resolution that is attainable for the wing membrane sample under 2-D MAS-DNP conditions. Unfortunately, contributions in the single-quantum spectral region 110–160 ppm are not observed in the DQ/SQ spectrum using SPC-5. The difficulty in observing resonances in the aromatic region for DQ/SQ experiments is common and is not unique to cicada membranes. Other MAS-DNP DQ/SQ experiments that have been previously developed [41–44] may enhance the signal contribution in the aromatic region for this type of sample and are being considered for future work.

Conclusions

The study of insect wings comes with great challenges. The life cycle of the insects, 17 years for the cicada, or the amount of sample available combined with the wings dissection, makes the study of these materials extremely challenging. While some species could potentially be isotopically labelled at significant cost, the vast majority cannot. Here we explored the relevance of MAS-DNP in this context.

We demonstrated that MAS-DNP can produce a high-quality ^{13}C CPMAS spectrum and a ^{13}C-^{13}C DQ/SQ correlation spectrum with only a 10 mg cicada wing membrane. 1-D CPMAS spectra can be obtained in just a few minutes. The 2-D correlation spectrum can be obtained in a reasonable amount of time and provides the resolution to resolve chitin resonances that overlap with resonances from protein. The observation of chitin in the cicada wing membrane contrasts with the chitin-free model of the insect wing membrane. The resolution of the SS-NMR spectra under DNP conditions is remarkable and we expect these promising results to be applicable to a wide variety of insect wings as well as other insect components, especially in cases where even a few milligrams of sample is difficult to acquire.

Acknowledgements

This work was partially supported by Grant CHE-1608149 from the NSF. A portion of this work was performed at the National High Magnetic Field Laboratory, which is supported by the National Science Foundation Cooperative Agreement No. DMR-1644779 and the state of Florida, the MAS-DNP instrument is supported by the NIH P41 GM122698 and NIH S10 OD018519. S.W. The Brood X (Knoxville, TN) cicada sloughs were kindly provided by Teresa Dyer. FMV thanks T. Halbritter and S. Sigurdsson who prepared and supplied c-AsymPol-POK.

References

1. Klowden MJ, Physiological Systems in Insects, Academic Press, New York, 2007.
2. Rajabi H, Dirks J-H, Gorb SN, Insect wing damage: causes, consequences, and compensatory mechanisms, J. Expt. Biol 223 (2020) 1–8.
3. Grimaldi D, Engel MS, Evolution of the Insects, Cambridge University Press, New York, 2005.
4. Pass G, Beyond aerodynamics: The critical roles of the circulatory and tracheal systems in maintaining insect wing functionality, Arthropod Struc. Dev 47 (2018) 391–407.
5. Wootton RJ, Functional morphology of insect wings, Annu. Rev. Entomol 37 (1992) 113–140.
6. Peter MG, Grun L, Forster H, CP/MAS-^{13}C-NMR spectra of sclerotized insect cuticle and chitin. Angew. Chem. Int. Ed 23 (1984) 638–639.

Author Manuscript Author Manuscript Author Manuscript Author Manuscript

7. Schaefer J, Kramer KJ, Garbow JR, Jacob GS, Stejskal EO, Hopkins TL, Speirs RD, Aromatic cross-links in insect cuticle: Detection by solid-state ^{13}C and ^{15}N NMR. Science 235 (1987) 1200–1204. [PubMed: 3823880]
8. Williams HJ, Scott AI, Woolfenden WR, Grant DM, Vinison SB, Elzen GW, Baehrecke EH, In vivo and solid state ^{13}C nuclear magnetic resonance studies of tyrosine metabolism during insect cuticle formation. Comp. Biochem. Physiol 89B (1988) 317–321.
9. Kramer KJ, Morgan TD, Hopkins TL, Christensen AM, Schaefer J, Solid-state ^{13}C-NMR and diphenol analysis of sclerotized cuticles from stored product coleoptera. Insect Biochem 19 (1989) 753–757.
10. Kramer KJ, Christensen AM, Morgan TD, T. D.; Schaefer, Czapla TH, Hopkins TL, Analysis of cockroach oothecae and exuviae by solid-state ^{13}C-NMR spectroscopy. Insect Biochem 21 (1991) 149–156.
11. Hopkins TL, Kramer KJ, Insect cuticle sclerotization. Annu. Rev. Entomol 37 (1992) 273–302.
12. Kramer KJ, Hopkins TL, Schaefer J, Applications of solids NMR to the analysis of insect sclerotized structures. Insect Biochem. Molec. Biol 25 (1995) 1067–1080.
13. Merritt ME, Christensen AM, Kramer KJ, Hopkins TL, Schaefer J, Detection of intercatechol cross-links in insect cuticle by solid-state carbon-13 and nitrogen-15 NMR. J. Am. Chem. Soc 118 (1996) 11278–11282.
14. Hopkins TL, Starkey SR, Xu R, Merritt ME, Schaefer J, Kramer KJ, Catechols involved in sclerotization of cuticle and egg pods of the grasshopper, *Melanoplus sanguinipes*, and their interactions with cuticular proteins. Arch. Insect Biochem. Physiol 40 (1999) 119–128.
15. Gullion JD, Gullion T, Solid-state NMR study of the cicada wing, J. Phys. Chem. B 121 (2017) 7646–7651. [PubMed: 28727439]
16. Eddy S, Gullion T, Characterization of insect wing membranes by ^{13}C CPMAS NMR, J. Phys. Chem. C 125 (2021) 931–936.
17. Maly T, Debelouchina GT, Bajaj VS, Hu K-N, Joo C-G, Mak–Jurkauskas ML, Sirigiri JR, van der Wel PCA, Herzfeld J, Temkin RJ, Griffin RG, Dynamic nuclear polarization at high magnetic fields. J. Chem. Phys 128(5), (2008) 052211.
18. Rossini AJ, Zagdoun A, Lelli M, Lesage A, Copéret C, Emsley L, Dynamic nuclear polarization surface enhanced NMR spectroscopy. Accts. Chem. Res 46(9) (2013) 1942–1951.
19. Ni QZ, Daviso E, Can TV, Markhasin E, Jawla SK, Swager TM, Temkin RJ, Herzfeld J, Griffin RG, High frequency dynamic nuclear polarization. Accts. Chem. Res 46(9) (2013) 1933–1941.
20. Lee D, Hediger S, De Paepe G, Is solid-state NMR enhanced by dynamic nuclear polarization? Sol. State Nucl. Magn. Reson 66–67 (2015) 6–20.
21. Rankin AGM, Trébosc J, Pourpoint F, Amoureux J-P, Lafon O, Recent developments in MAS DNP-NMR of materials. Sol. State Nucl. Magn. Reson 101 (2019) 116–143.
22. Thankamony ASL, Wittmann JJ, Kaushik M, Corzilius B, Dynamic nuclear polarization for sensitivity enhancement in modern solid-state NMR. Prog. Nucl. Magn. Reson. Spec 102–103 (2017) 120–195.
23. Takahashi H, Lee D, Dubois L, Bardet M, Hediger S, De Paepe G, Rapid NaturalAbundance 2D ^{13}C- ^{13}C correlation spectroscopy using dynamic nuclear polarization enhanced solid-state NMR and matrix-free sample preparation. Angew. Chem. Inter. Ed 51(47) (2012) 11766–11769.
24. Rossini AJ, Zagdoun A, Hegner F, Schwarzwälder M, Gajan D, Copéret C, Lesage A, Emsley L, Dynamic nuclear polarization NMR spectroscopy of microcrystalline solids. J. Am. Chem. Soc 134(40) (2012) 16899–16908. [PubMed: 22967206]
25. Takahashi H, Hediger S, De Paepe G, Matrix-free dynamic nuclear polarization enables solid-state NMR ^{13}C–^{13}C correlation spectroscopy of proteins at natural isotopic abundance. Chem. Comm 49(82) (2013) 9479.
26. Smith AN, Märker K, Hediger S, De Paepe G, Natural isotopic abundance ^{13}C and ^{15}N multidimensional solid-state NMR enabled by dynamic nuclear polarization. J. Phys. Chem. Lett 10(16) (2019) 4652–4662. [PubMed: 31361489]
27. Craig HC, Blamires SJ, Sani M-A, Kasumovic MM, Rawal A, Hook JM, DNP NMR spectroscopy reveals new structures, residues and interactions in wild spider silks. Chem. Comm 55 (2019) 4687–4690. [PubMed: 30938741]

Author Manuscript Author Manuscript Author Manuscript Author Manuscript

28. Zhao W, Kirui A, Deligey F, Mentink-Vigier F, Zhou Y, Zhang B, Wang T, Solid-state NMR of unlabeled plant cell walls: high-resolution structural analysis without isotopic enrichment. Biotech. Biofuels Bioprod, 14(1) (2021) 14.
29. Perras FA, Luo H, Zhang X, Mosier NS, Pruski M, Abu-Omar MM, Atomic-level structure characterization of biomass pre- and post-lignin treatment by dynamic nuclear polarization-enhanced solid-state NMR. J. Phys. Chem. A 121 (2017) 623–630. [PubMed: 28026949]
30. Geiger Y, Gottlieb HE, Akbey U, Oschkinat H, Goobes G, Studying the conformation of a silaffin-derived pentalysine peptide embedded in bioinspired silica using solution and dynamic nuclear polarization magic-angle spinning NMR, J. Am. Chem. Soc 138 (2016) 5561–5567. [PubMed: 26451953]
31. Sajomsang W, Gonil P, Preparation and characterization of α-chitin from cicada sloughs, Mat. Sci. Eng. C 30 (2010) 357–363.
32. Harrabi R, Halbritter T, Aussenac F, Dakhlaoui O, Tol J, Damodaran KK, Lee D, Paul S, Hediger S, Mentink-Vigier F, Sigurdsson ST, De Paepe G, Highly efficient polarizing agents for MAS-DNP of proton-dense molecular solids. Angew. Chem. Intern. Ed 61 (2022) e202114103.
33. Dubroca T, Smith ANAN, Pike KJKJ, Froud S, Wylde R, Trociewitz B, McKay JE, Mentink-Vigier F, van Tol J, Wi S, Brey WW, Long JR, Frydman L, Hill S, A quasi-optical and corrugated waveguide microwave transmission system for simultaneous dynamic nuclear polarization NMR on two separate 14.1 T spectrometers. J. Magn. Reson 289 (2018) 35–44. [PubMed: 29459343]
34. Thurber KR, Tycko R, Low-temperature dynamic nuclear polarization with helium-cooled samples and nitrogen-driven magic-angle spinning. J. Magn. Reson 264 (2016) 99–106. [PubMed: 26920835]
35. Fung BM, Khitrin AK, Ermolaev K, An improved broadband decoupling sequence for liquid crystals and solids. J. Magn. Reson 142(1) (2000) 97–101. [PubMed: 10617439]
36. Hohwy M, Rienstra CM, Jaroniec CP, Griffin RG, Fivefold symmetric homonuclear recoupling in rotating solids: Application to double quantum spectroscopy, J. Chem. Phys 110 (1999) 7983–7992.
37. Goularte NF, Kallem T, Cegelski L, Chemical and molecular composition of the chrysalis reveals common chitin-rich structural framework for monarchs and swallowtails, J. Molec. Biol 434 (2022) 167456.
38. Johnson RL, Schmidt-Rohr K, Quantitative solid-state ^{13}C NMR with signal enhancement by multiple cross polarization, J.Magn. Reson 239 (2014) 44–49. [PubMed: 24374751]
39. Fernando LD, Zhao W, Dickwella Widanage MC, Mentink-Vigier F, Wang T, Solid-state NMR and DNP investigations of carbohydrates and cell-wall materials, eMagRes 9(3) (2020)
40. van der Wel PCA, Hu K-N, Lewandowski JR, Griffin RG, Dynamic nuclear polarization of amyloidogenic peptide nanocrystals: GNNQQNY, a core segment of the yeast prion protein, J. Am. Chem. Soc 128 (2006) 10840–10846. [PubMed: 16910679]
41. Teymoori G, Pahari B, Stevensson B, Edén M, Low-power broadband homonuclear dipolar recoupling without decoupling: Double-quantum ^{13}C NMR correlations at very fast magic-angle spinning, Chem. Phys. Lett 547 (2012) 103–109.
42. Teymoori G, Pahari B and Edén MLow-power broadband homonuclear dipolar recoupling in MAS NMR by two-fold symmetry pulse schemes for magnetization transfers and double-quantum excitation, J. Magn. Reson 261 (2015) 205–220. [PubMed: 26515279]
43. Märker K, Paul S, Fernández-de-Alba C, Lee D, Mouesca J-M, Hediger S, De Paepe G, Welcoming natural isotopic abundance in solid-state NMR: probing π-stacking and supramolecular structure of organic nanoassemblies using DNP. Chemical Science, 8(2) (2017) 974–987. [PubMed: 28451235]
44. Wi S, Dwivedi N, Dubey R, Mentink-Vigier F, Sinha N, Dynamic nuclear polarization-enhanced, double-quantum filtered ^{13}C-^{13}C dipolar correlation spectroscopy of natural ^{13}C abundant bone-tissue biomaterial, J. Magn. Reson 335 (2022) 107144.

Author Manuscript Author Manuscript Author Manuscript Author Manuscript

Highlights

- Insect wing membranes are composite materials made of chitin and protein
- Macromolecular components of the insect wing membrane are identified by NMR
- MAS-DNP provides signal enhancement and resolution to characterize insect wing membranes

Author Manuscript Author Manuscript Author Manuscript Author Manuscript

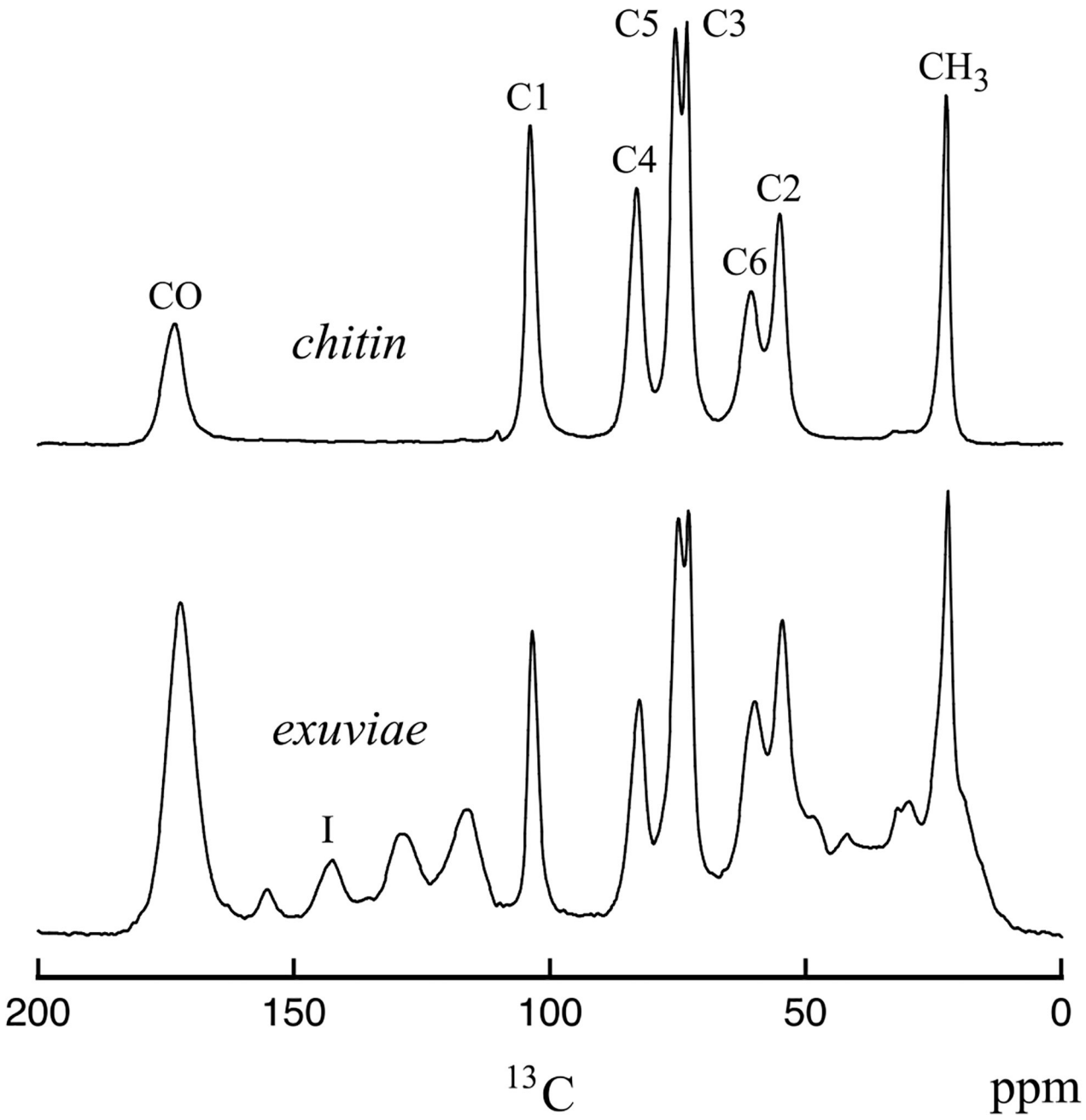

Figure 1.

^{13}C CPMAS spectra of cicada exuviae (bottom) and chitin obtained from cicada exuviae (top). The spectra were obtained at room temperature on the 151 MHz (proton) spectrometer. The resonances shown in the chitin spectrum are labeled according to the chitin carbon positions for the structure shown in Table 1. The resonance labeled I in the exuviae spectrum arises from catechols.

Author Manuscript Author Manuscript Author Manuscript Author Manuscript

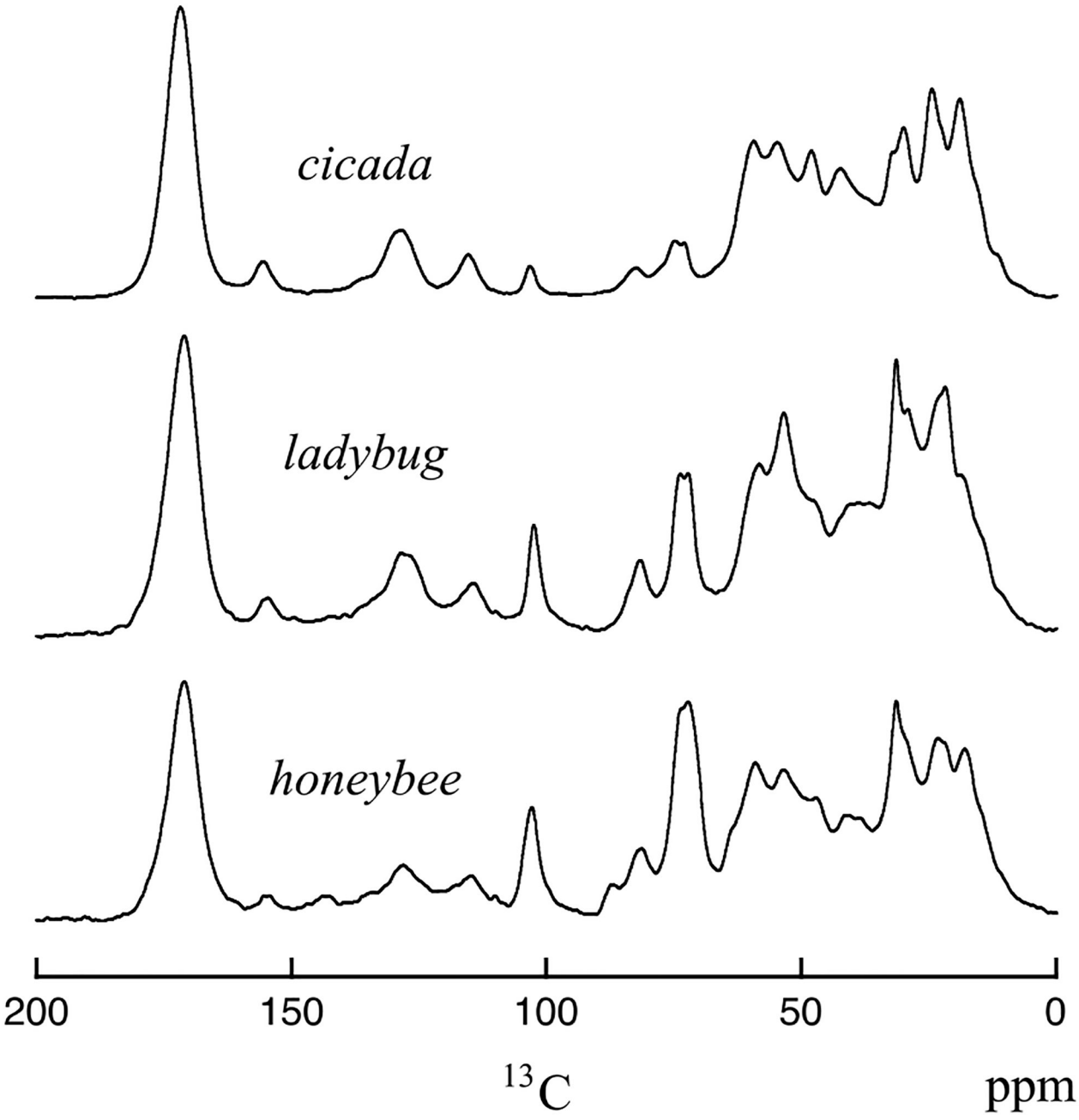

Figure 2.
^{13}C CPMAS spectra of wing membranes for cicada, ladybug, and honeybee. The spectra were obtained at room temperature on the 151 MHz (proton) spectrometer.

Author Manuscript Author Manuscript Author Manuscript Author Manuscript

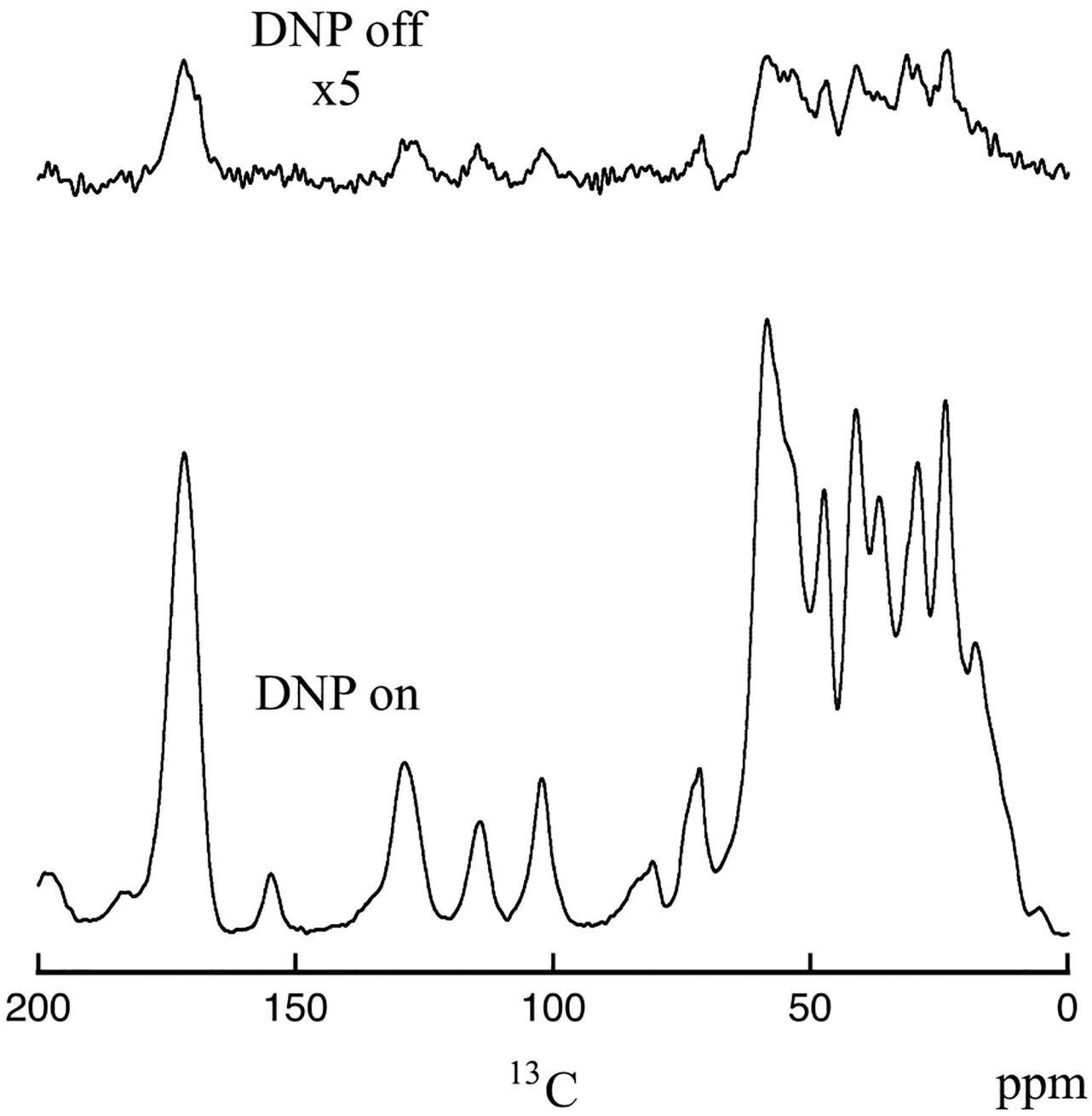

Figure 3.

^{13}C CPMAS spectra of cicada wing membrane with DNP on (bottom) and DNP off (top). The spectra were obtained on the 600 MHz (proton) MAS-DNP spectrometer collected with a sample spinning speed of 10.5 kHz.

Author Manuscript Author Manuscript Author Manuscript Author Manuscript

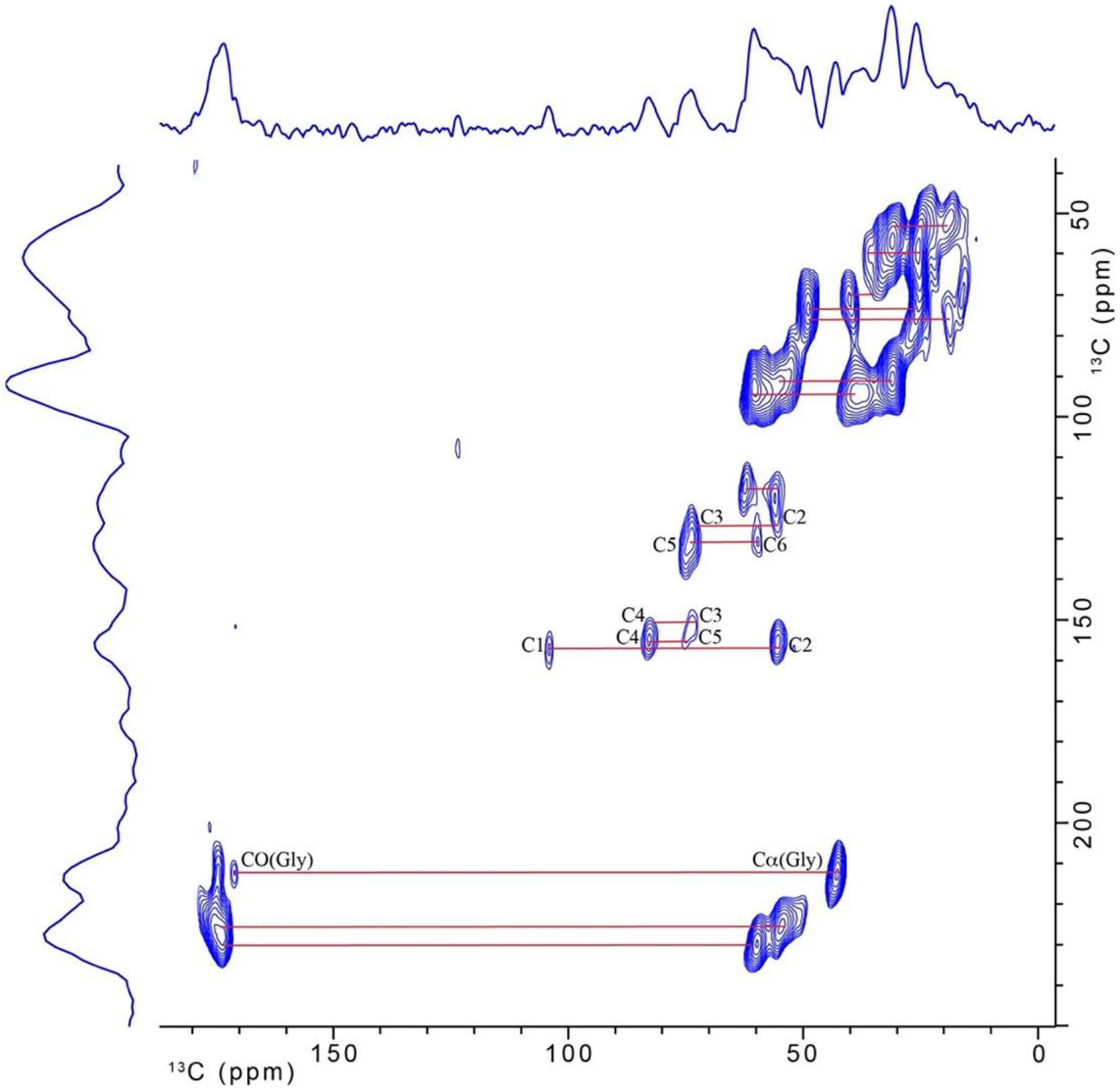

Figure 4.

^{13}C-^{13}C double-quantum/single-quantum spectrum for cicada wing membrane. The spectrum was obtained on the 600 MHz (proton) MAS-DNP spectrometer.

Author Manuscript

Author Manuscript

Author Manuscript

Author Manuscript

Table 1.

^{13}C isotropic chemical shifts for components common to insect cuticle. The original values for cuticle components from the Schaefer *et al.* paper appear in the table [7]. A similar table was published by Peter *et al.* [6]. The repeat unit for chitin, along with carbon position labels, is shown for reference.

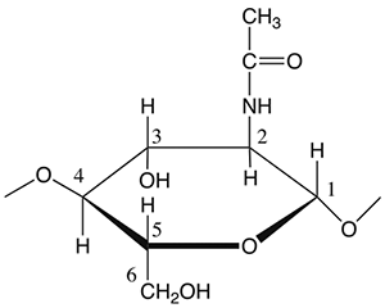

^{13}C resonance position (ppm)	Assignment
172	Carbonyl carbons of chitin, protein, lipid, and catechol acyl groups
170	Carbonyl carbons of oxalate
155	Phenoxy carbon of tyrosine, guanidino carbons in arginine
144	Phenoxy carbons of catechols
129	Aromatic carbons
116	Tyrosine carbons 3 and 5, imidazole carbon 4, catechol carbons 2 and 5
104	Chitin carbon 1
82	Chitin carbon 4
75	Chitin carbon 5
72	Chitin carbon 3
60	Chitin carbon 6, amino acid α-carbons
55	Chitin carbon 2, amino acid α-carbons
44	Aliphatic carbons of amino acids, catechols, and lipids
33	Aliphatic carbons of amino acids, catechols, and lipids
30	Aliphatic carbons of lipids
23	Methyl carbons of chitin, protein, lipid, and catechol acyl groups; amino acid methyne carbons
19	Methyl carbons of amino acids and lipids